Heliyon 10 (2024) e30688

Contents lists available at ScienceDirect

Heliyon

journal homepage: www.cell.com/heliyon

Research article

Modification of MgH_2 hydrogen storage performance by nickel-based composite catalyst Ni/NiO

Wenxuan Li [a], Xinglin Yang [a,*], Quanhui Hou [b], Xiaohui Lu [a], Jie Kong [a], Jianye Su [a]

[a] School of Energy and Power, Jiangsu University of Science and Technology, Zhenjiang, 212003, China
[b] School of Automotive Engineering, Yancheng Institute of Technology, Yancheng, 224051, China

ARTICLE INFO

Keywords:
MgH_2
Hydrogen storage performance
Modification
Ni/NiO

ABSTRACT

In this study, the Ni/NiO catalyst was demonstrated to enhance the hydrogen storage performance of MgH_2. The dehydrogenation of MgH_2+10 wt% Ni/NiO started at approximately 180 °C, achieving 5.83 wt% of dehydrogenation within 10 min at 300 °C. Completely dehydrogenated, MgH_2 began to rehydrogenate at about 50 °C, absorbing about 4.56 wt% of hydrogen in 10 min at 150 °C. In addition, the activation energies of dehydrogenation and rehydrogenation of MgH_2+10 wt% Ni/NiO were 87.21 and 34.84 kJ/mol. During the dehydrogenation/rehydrogenation cycle, Mg_2Ni/Mg_2NiH_4 could promote hydrogen diffusion, thus enhancing the hydrogen storage performance of Mg/MgH_2.

1. Introduction

Energy is an indispensable part of human life. However, the extensive use of fossil energy sources has resulted in an escalating energy predicament and environmental degradation. Hydrogen is a promising alternative to fossil fuels because of its elevated fuel effectiveness and ecological benevolence (the combustion product is water) [1]. However, hydrogen containment currently poses a pivotal challenge in advancing hydrogen energy. Solid hydrogen storage materials, which offer high safety and heightened hydrogen density while capable of containing hydrogen under low pressure, have attracted much attention [2].

MgH_2, distinguished by its elevated hydrogen storage capability and favorable reversibility, emerges prominently among numerous solid hydrogen storage substances. Nevertheless, the pragmatic advancement of MgH_2 faces impediments due to its considerable thermodynamic stability and sluggish kinetics in the dehydrogenation/rehydrogenation processes [3]. Many studies have demonstrated that catalyst doping can significantly improve the kinetic properties of Mg/MgH_2, leading to its rapid dehydrogenation/rehydrogenation at low temperatures.

Currently, various types of transition metals (e.g., Ni [4], Fe [5], Ti [6]) and their constituent metal alloys (e.g., Ni_3Fe [7], CoFeB [8]), metal compounds (e.g., FeOOH [9], TiO_2 [10]), and metal composites (e.g., the complexes of carbon materials with Ni——Ni@C [11], graphene-supported TiNiFe [12]) have been widely used to improve the hydrogen storage properties of Mg/MgH_2. In contrast to alternative transition metals, Ni is cost-effective and demonstrates the capacity to enhance the hydrogen storage characteristics of Mg/MgH_2, drawing considerable interest from researchers.

Rahwanto et al. [4] found that the incorporation of 2 mol% Ni resulted in 5.3 wt% hydrogen uptake by Mg/MgH2 within 5 min at

* Corresponding author.
E-mail addresses: liwenxuan4084@163.com (W. Li), yangxl23320@163.com (X. Yang), hqhdyx66@ycit.edu.cn (Q. Hou), xiaohuilu6@163.com (X. Lu), 221210801120@stu.just.edu.cn (J. Kong), sujianye2022@163.com (J. Su).

https://doi.org/10.1016/j.heliyon.2024.e30688
Received 15 February 2024; Received in revised form 1 May 2024; Accepted 2 May 2024
Available online 4 May 2024

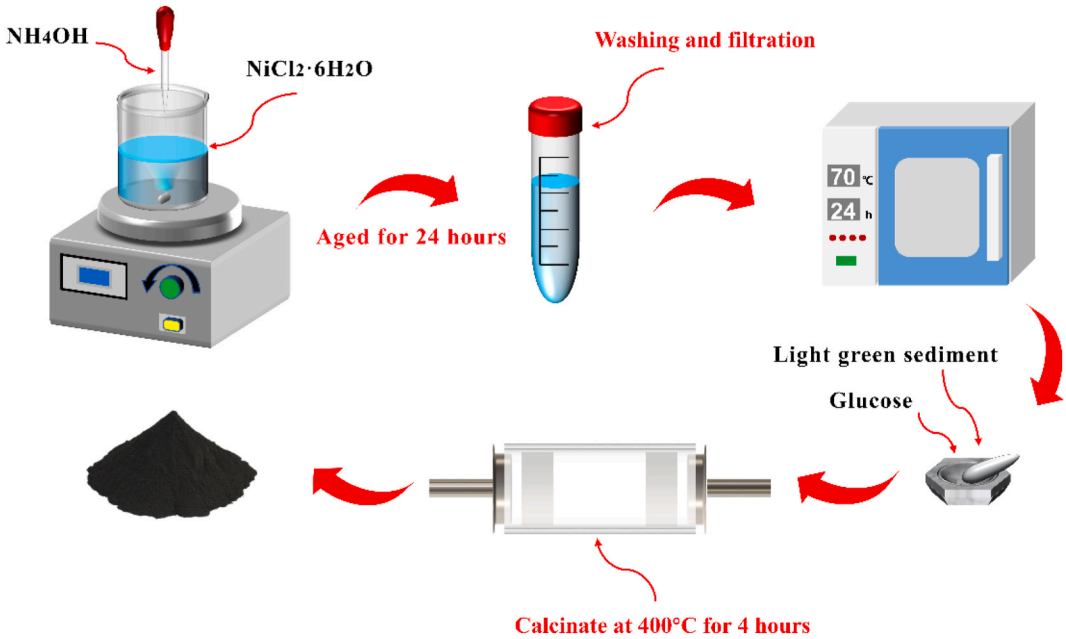

Fig. 1. Schematic diagram of the preparation process of Ni/NiO catalyst.

300 °C and was able to complete dehydrogenation within 4 min at 50 mbar. In addition, Dan et al. [13] discovered that the dehydrogenation/rehydrogenation kinetics of Mg/MgH_2 were significantly enhanced by compositing 2–6 nm nickel nanoparticles with MgH_2, and MgH_2-Ni exhibited rapid dehydrogenation, releasing more than 6.5 wt% at 275 °C within 10 min. This enhancement was attributed to $Mg_2NiH_{0.3}$ during dehydrogenation/rehydrogenation cycling.

Not only that, building upon the foundation of nickel, researchers have devised a variety of nickel-based compounds (e.g., NiB [14], NiO [15]) or nickel-based composites (e.g., Ni/Fe_3O_4@MIL [16], NiO@$KNbO_3$ [17]) to enhance the kinetic of the dehydrogenation/rehydrogenation process of Mg/MgH_2. Liu et al. [14] observed significant improvement in the kinetic properties of MgH_2 by adding 10 wt% NiB, and MgH_2-10 wt% NiB demonstrated the release of 6.0 wt% hydrogen within 10 min at 300 °C. In addition, Zhang et al. [15] explored compound catalysts, including NiO, Ni_3C, Ni_3N, Ni_2P, etc. The experimental findings indicated that all these catalysts exhibited commendable catalytic effects.

Based on the element nickel, various nickel-based composites developed by scholars have likewise exhibited good catalytic properties [16–21]. For example, Ren et al. [16] prepared Ni/Fe_3O_4@MIL based on nickel and found that at 598 K, MgH_2-Ni/-Fe_3O_4@MIL could dehydrogenate about 3.3 wt% in 10 min. In addition, Hou et al. [20] found that MgH_2+10 wt% Ni/BC-3 commenced hydrogen liberation at 187.8 °C. At 300 °C, MgH_2+10 wt% Ni/BC-3 can dehydrogenate about 6.3 wt% in 5 min. It is worth mentioning that Hou's team developed Ni/BC-3 based on Ni and NiO/C based on NiO. It was demonstrated that the incorporation of 9 wt% NiO/C resulted in a 155 °C decrease in the initial dehydrogenation temperature of MgH_2. Moreover, MgH_2+9 wt% NiO/C could dehydrogenate 6.21 wt% at 300 °C for 10 min [21]. Wu et al. [17] observed a reduction of 111 °C in the initial dehydrogenation temperature of MgH_2, decreasing from the original 286 °C–175 °C, adding 5 wt% NiO@$KNbO_3$. Additionally, at 300 °C, MgH_2-5wt% NiO@$KNbO_3$ demonstrated the release of 3.92 wt% within 10 min. These studies show that Ni or NiO with good catalytic properties can be combined with more active catalytic substances to form high-quality, high-performance catalysts to boost the hydrogen storage capabilities of Mg/MgH_2.

Considering the excellent modification ability of Ni and NiO and their composites to Mg/MgH_2, there is no research on catalysts combining Ni and NiO. It was decided to prepare a catalyst combining Ni and NiO's advantages to enhance the hydrogen storage capabilities of Mg/MgH_2. In this study, Ni/NiO was synthesized using the co-precipitation method, and its impact on the hydrogen storage capabilities of Mg/MgH_2 was investigated.

2. Experimental

2.1. Synthesis of Ni/NiO

The synthesis process of the Ni/NiO catalyst is based on the relevant literature that has been reported [22]. First, NH_4OH was added dropwise to a 10% mass fraction of $NiCl_2{\cdot}6H_2O$ solution, stirred constantly until the pH of the solution reached 11, and the mixture was aged for 24 h. Then, the light green sediment produced by the mixture was washed with deionized water and anhydrous ethanol, respectively, and filtered, and the sediment was dried at 70 °C. Finally, the dried sediment was mixed and ground with glucose in a mortar at a mass ratio of 1:2, and then the mixture was calcined in a covered crucible at 400 °C for 4 h to obtain a Ni/NiO catalyst. The

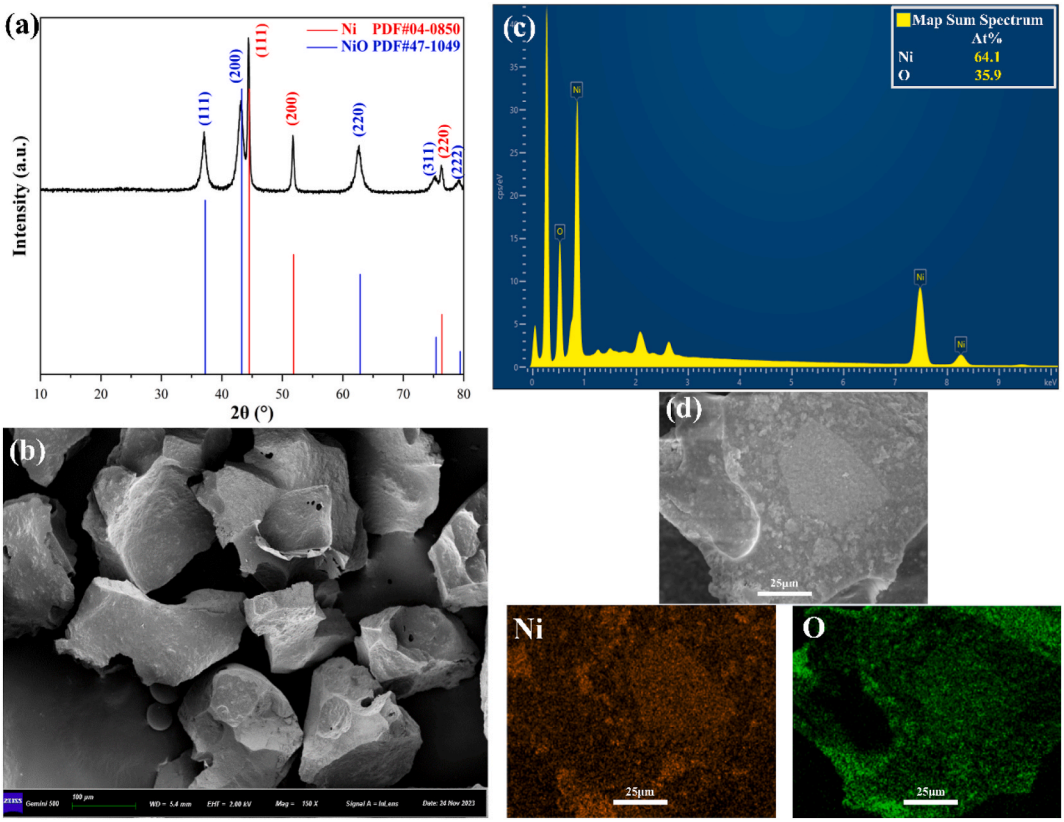

Fig. 2. XRD image (a), SEM image (b), EDS images (c, d) of Ni/NiO catalyst.

prepared catalyst was placed in a glove box before use. Fig. 1 briefly shows the preparation steps of the Ni/NiO catalyst.

2.2. Preparation of MgH_2+Ni/NiO

First, the Mg powder was hydrogenated at a hydrogen pressure of 70 bar and 380 °C for 2 h. Subsequently, the MgH_2 powder was placed into a ball mill jar and ball-milled at a rotational speed of 450 r/min for 5 h in a planetary ball mill. After the ball milling, the sample was hydrogenated again under the same conditions as the first time. Next, the sample was ball-milled at 450 r/min for 5 h and pounded every 1 h. Finally, the sample was subjected to the last hydrogenation under hydrogenation conditions consistent with the first time. After these operations, the MgH_2 powder was successfully prepared.

MgH_2 and Ni/NiO were mixed into ball mills in an argon atmosphere according to mass ratios of 95:5, 90:10, and 85:15 and mixed at a rotational speed of 450 r/min for 2 h. After ball milling, the samples were pounded and collected, recorded as MgH_2+5 wt% Ni/NiO, MgH_2+10 wt% Ni/NiO, and MgH_2+15 wt% Ni/NiO, respectively. All samples were processed in a glove box with water and oxygen concentrations below 0.1 ppm.

3. Results and discussions

3.1. Characterization of Ni/NiO

The XRD of the Ni/NiO catalyst is shown in Fig. 2(a), where two different colors of diffraction peaks can be found. The red diffraction peaks are typical of Ni (PDF#04-0850), and it can be seen that there are robust diffraction features at $2\theta = 44.507°$, 51.846°, and 76.370°, aligning with the (111), (200) and (220) lattice planes, respectively. In addition, the blue diffraction peaks are typical of NiO (PDF#47-1049), and the diffraction peaks mainly appear at $2\theta = 37.248°$, 43.275°, and 62.878°, corresponding to the (111), (200), and (220) lattice planes, respectively. Fig. 2(b) shows that the Ni/NiO catalyst exhibits a large-scale, micron-scale irregular structure. Fig. 2 (c, d) shows the elemental composition of the catalyst as Ni and O, and their relative elemental contents are 64.1% and 35.9%, respectively.

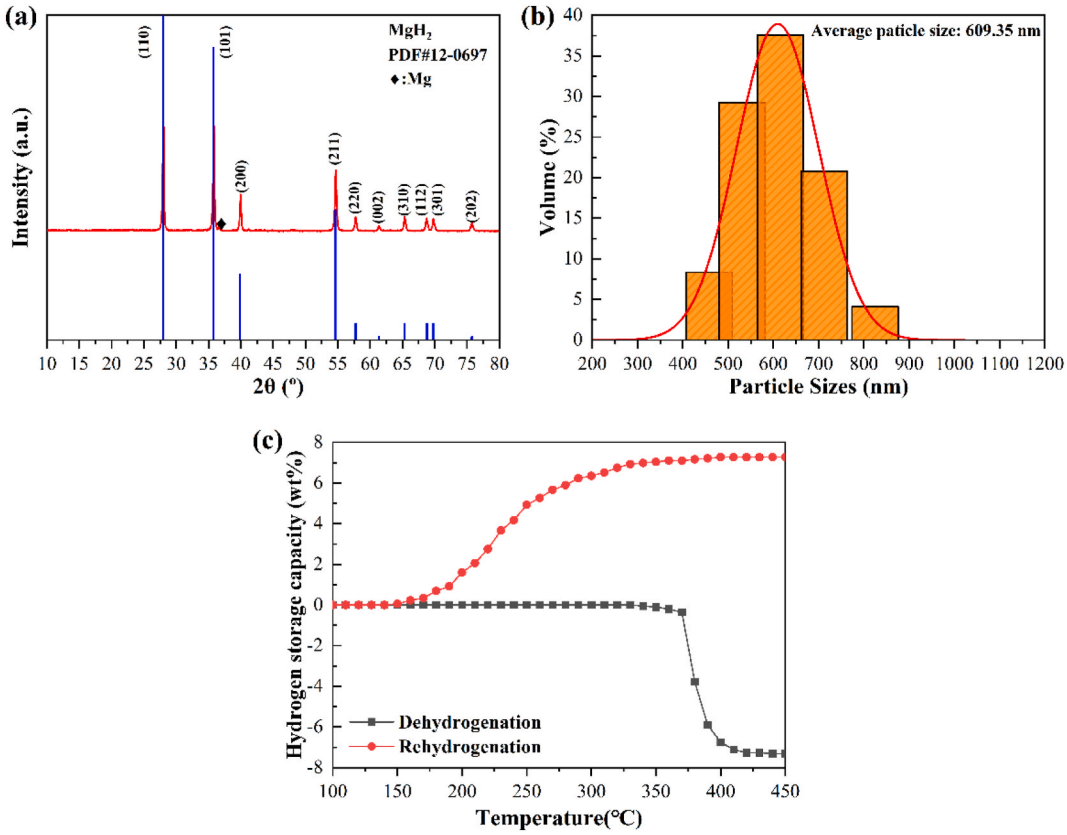

Fig. 3. XRD (a), PSDA (b), and hydrogen storage performance test chart (c) of MgH_2.

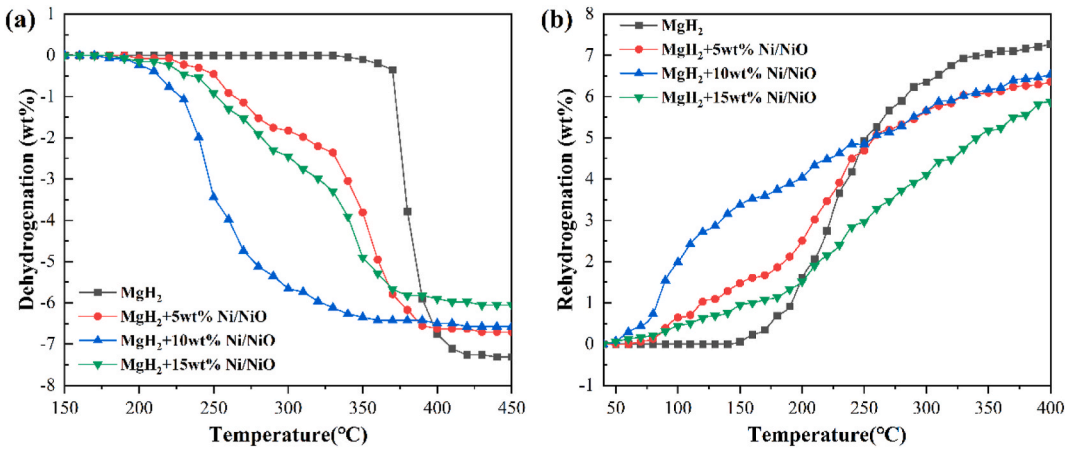

Fig. 4. Heating dehydrogenation plots (a) and heating rehydrogenation plots (b) of pure MgH_2, MgH_2+5 wt% Ni/NiO, MgH_2+10 wt% Ni/NiO and MgH_2+15 wt% Ni/NiO.

3.2. *Characterization and testing of MgH_2*

To verify the authenticity and validity of the homemade MgH_2, XRD and PSDA characterization were performed, as illustrated in Fig. 3(a) and (b). The diffraction features of XRD are in complete agreement with the standard card for MgH_2 (PDF#12-0697), which indicates that the preparation of MgH_2 was successful. Fig. 3(b) shows that the particle dimensions of MgH_2 vary between 400 and 900 nm, with a mean particle size of 609.35 nm. Fig. 3(c) shows the dehydrogenated and rehydrogenated properties of pure MgH_2. MgH_2 exhibited a dehydrogenation onset temperature of approximately 340 °C, and the hydrogen absorption temperature was about 150 °C.

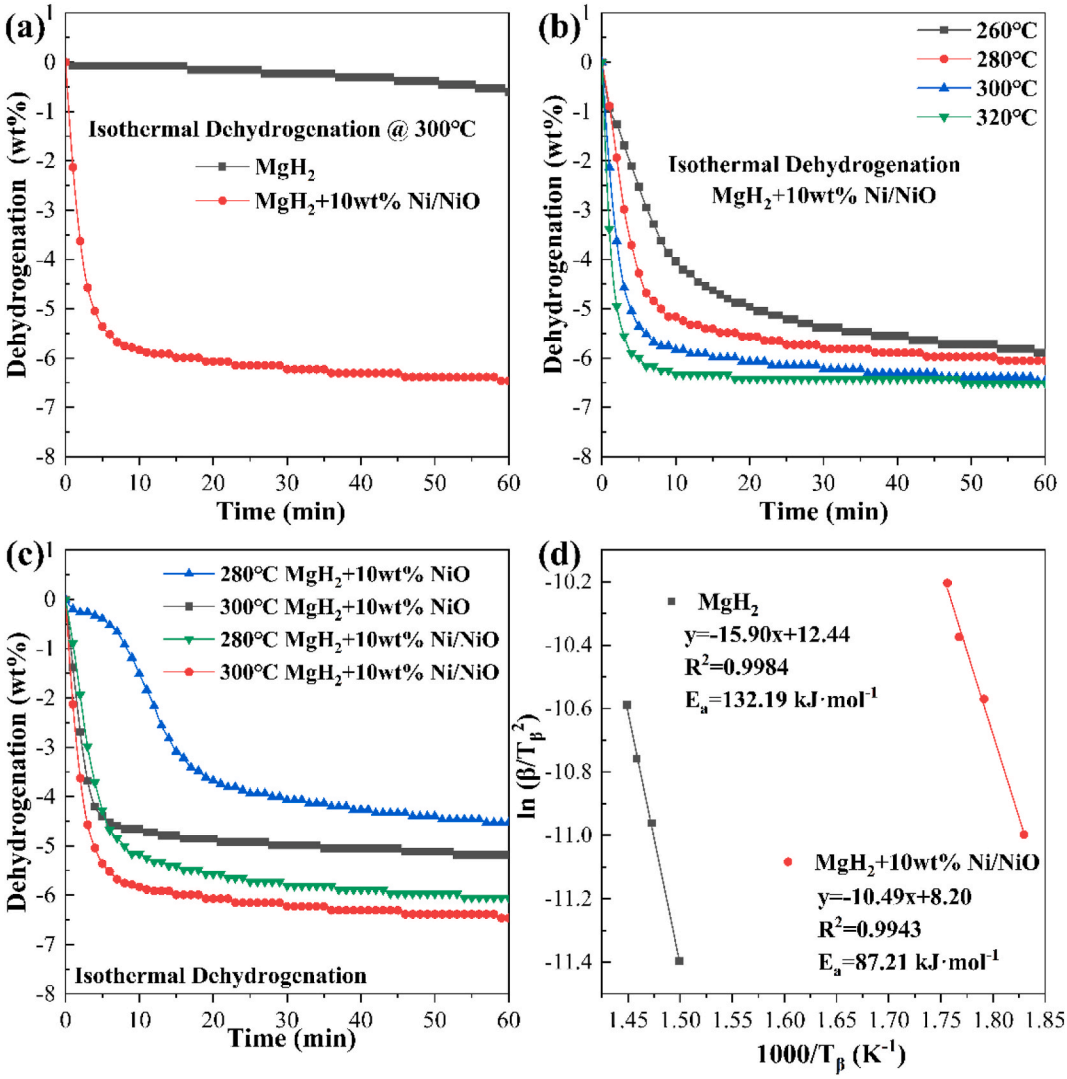

Fig. 5. Isothermal dehydrogenation profiles of pure MgH_2 and MgH_2+10 wt% Ni/NiO at 300 °C (a), isothermal dehydrogenation profiles of MgH_2+10 wt% Ni/NiO at different temperatures (b), isothermal dehydrogenation profiles of MgH_2+10 wt% NiO and MgH_2+10 wt% Ni/NiO at 280 °C and 300 °C (c) and dehydrogenated activation energy of pure MgH_2 and MgH_2+10 wt% Ni/NiO (d).

The final dehydrogenation and rehydrogenation could reach about 7.31 wt% and 7.27 wt%, respectively, reaching 96.2% and 95.7% of the theoretical value (7.6 wt%).

3.3. Preliminary exploration of the dehydrogenation/rehydrogenation performance of MgH_2+Ni/NiO

Fig. 4(a) shows the influence of various ratios of Ni/NiO catalysts on the dehydrogenation efficacy of MgH_2. The dehydrogenation temperature after Ni/NiO doping was significantly reduced compared with pure MgH_2. The effect of 10 wt% Ni/NiO was the most significant, and its introduction reduced the initiation temperature of MgH_2 dehydrogenation from around 340 °C–180 °C. The doping of 5 wt% Ni/NiO and 15 wt% Ni/NiO resulted in the dehydrogenation of MgH_2 at 200 °C and 190 °C, with final dehydrogenation amounts of 6.71 wt% and 6.05 wt%, respectively. It is worth mentioning that the dehydrogenation rate of MgH_2+10 wt% Ni/NiO was very rapid, with 6.42 wt% dehydrogenation at 360 °C, reaching 97.7% of the total dehydrogenation (6.57 wt%). Fig. 4(b) shows the rehydrogenation performance of the MgH_2+Ni/NiO. The introduction of Ni/NiO significantly reduced the reabsorption temperature of MgH_2. The temperature for reabsorption of hydrogen by MgH_2 was approximately 150 °C, and the composite could start reabsorption at 50 °C after adding the Ni/NiO catalyst. After hydrogen reabsorption, the hydrogen reabsorption of MgH_2+10 wt% Ni/NiO could reach 6.54 wt%, while the reabsorption of MgH_2+15 wt% Ni/NiO could reach 5.87 wt%. From the view of total hydrogen storage, the hydrogen storage capacities of MgH_2+5 wt% Ni/NiO and MgH_2+10 wt% Ni/NiO were highly similar. However, the dehydrogenation/rehydrogenation rate of MgH_2+10 wt% Ni/NiO was more significant. Considering the dehydrogenation/rehydrogenation

Table 1
The dehydrogenation activation energy of Mg/MgH_2 hydrogen storage systems doped with different nickel-based catalysts.

Hydrogen storage systems	E_a (kJ/mol)	Ref.
MgH_2+10 wt% Ni/NiO	87.21	This work
MgH_2+10 wt% Ni@C	93.08	[11]
MgH_2+5 wt% Ni_3C	97.8	[15]
MgH_2+10 wt% $ZrNi_5$	110.06	[27]
MgH_2+10 wt% $NiMoO_4$	119.47	[28]
MgH_2+Ni_3S_2@C-4	115.2	[29]
MgH_2+10 wt% CrFeCoNi	133.06	[30]
MgH_2+10 wt% $TiMgVNi_3$	94.42	[31]

characteristics of MgH_2+Ni/NiO, MgH_2+10 wt% Ni/NiO was used for further research.

3.4. Further exploration of the dehydrogenation/rehydrogenation performance of MgH_2+10 wt% Ni/NiO

In Fig. 5(a), the dehydrogenation rate of MgH_2 at 300 °C was prolonged, with only 0.60 wt% dehydrogenation in 60 min. However, under the same condition, the dehydrogenation rate of MgH_2+10 wt% Ni/NiO was very significant, with about 5.83 wt% dehydrogenation in 10 min and a total dehydrogenation of 6.46 wt%. Compared with previous reports, MgH_2-NiO could dehydrogenate 4.1 wt % in 20 min at 300 °C [15]. The dehydrogenation of MgH_2+9 wt% Ni could reach 6.3 wt% in 2.5min at 300 °C [23]. Furthermore, MgH_2 doped with catalyst $MgCCo_{1.5}Ni_{1.5}$ released about 5 wt% hydrogen within 10 min at 325 °C [24]. MgH_2 doped with Ni-50%Cu released about 5.14 wt% hydrogen in 15 min at 300 °C [25]. MgH_2 doped with 10 wt% Ni@C released about 4.8 wt% within 10 min at 300 °C [11]. Fig. 5(b) shows that the total amount and rate of dehydrogenation of MgH_2+10 wt% Ni/NiO increased effectively with the increase in temperature. Under the condition of 260 °C, the dehydrogenation of MgH_2+10 wt% Ni/NiO could reach 5.38 wt% within 30min.

In this paper, the excellent performance of the Ni/NiO catalyst was further verified by the comparative experiments in Fig. 5(c). With the increase in temperature, although the dehydrogenation rate of MgH_2+10 wt% NiO was improved, it still needed to be improved compared to that of MgH_2+10 wt% Ni/NiO. It is worth mentioning that the dehydrogenation of MgH_2+10 wt% NiO was only 5.18 wt% in 60 min at 300 °C, which was not as good as the dehydrogenation (5.24 wt%) of MgH_2+10 wt% Ni/NiO in 12 min at 280 °C. It can be seen that the Ni/NiO catalyst formed by combining Ni and NiO has a better catalytic performance than NiO, and the introduction of Ni may help improve NiO's catalytic effect, which is a crucial point to be explored in future research.

The activation energy for dehydrogenation in pure MgH_2 and MgH_2+10 wt% Ni/NiO calculated by combining the Kissinger formula [26] is depicted in Fig. 5(d). The activation energy of pure MgH_2 was recorded at 132.19 kJ/mol, which decreased to 87.21 kJ/mol following the incorporation of 10 wt% Ni/NiO. Therefore, adding 10 wt% Ni/NiO enhanced the dehydrogenation reaction of MgH_2, decreased its dehydrogenation temperature and activation energy and enhanced its dehydrogenation rate. Table 1 shows the dehydrogenation activation energy of Mg/MgH_2 hydrogen storage systems doped with nickel-based materials.

For MgH_2+10 wt% Ni/NiO, the constant temperature rehydrogenation performance test is also critical. Fig. 6(b) shows the continuous temperature rehydrogenation performance of fully dehydrogenated MgH_2+10 wt% Ni/NiO within 60 min. The fully dehydrogenated MgH_2+10 wt% Ni/NiO had a reasonable hydrogen uptake rate at 150 °C, with reabsorption up to 5.35 wt% in 60 min. Even when the temperature was reduced to 100 °C, the fully dehydrogenated MgH_2+10 wt% Ni/NiO could still absorb 4.29 wt% of hydrogen. As a comparison, the completely dehydrogenated MgH_2 was tested for constant temperature reabsorption at various temperatures, and the outcomes are presented in Fig. 6(a). When the temperature exceeded 210 °C, the reabsorption of hydrogen by MgH_2 was comparable to that of MgH_2+10 wt% Ni/NiO. Incorporating Ni/NiO catalyst enhanced the hydrogen reuptake kinetics of MgH_2. The activation energy for hydrogen absorption is a crucial parameter characterizing the kinetic of hydrogen reuptake. Data from constant temperature hydrogen reabsorption was utilized as the foundational parameter, and the curves were fitted with the help of the JMAK equation [26], as depicted in Fig. 6(c) and (d). The curves at different temperatures have a good fit. The Arrhenius equation [30] was used to calculate the activation energy of the hydrogen uptake. Fig. 6(e) illustrates that the two curves exhibited strong fits, one at 0.999 and the other at 0.994. The activation energies of pure MgH_2 and MgH_2+10 wt% Ni/NiO were 68.36 and 34.84 kJ/mol. Introducing Ni/NiO reduced the reabsorption temperature of fully dehydrogenated MgH_2, greatly reduced its reaction energy barrier, and significantly improved its rehydrogenation kinetic. Table 2 shows the hydrogen absorption activation energy of the Mg/MgH_2 hydrogen storage systems doped with nickel-based materials.

3.5. Study on the stability of the dehydrogenation/rehydrogenation cycle of MgH_2+10 wt% Ni/NiO

To explore the cycling stability of MgH_2+10 wt% Ni/NiO, 10 dehydrogenation/rehydrogenation cycles were tested under hydrogen at 3 MPa and 320 °C, as depicted in Fig. 7. The extent of hydrogen release and rehydrogenation during the initial cycle was 6.34 wt% and 6.01 wt%. At the end of the third cycle, the dehydrogenation value of the composite decayed from 6.34 wt% to 5.90 wt%, a decrease of 0.44 wt%. Within the subsequent seven cycles, the dehydrogenation value of the composite decayed from 5.90 wt% to 5.72 wt%, a decrease of only 0.18 wt%. This suggests that the dehydrogenation of the composite stabilized at the end of the third cycle. In addition, in the first cycle, the rehydrogenation value of the composite was 0.33 wt% less than the dehydrogenation value. However,

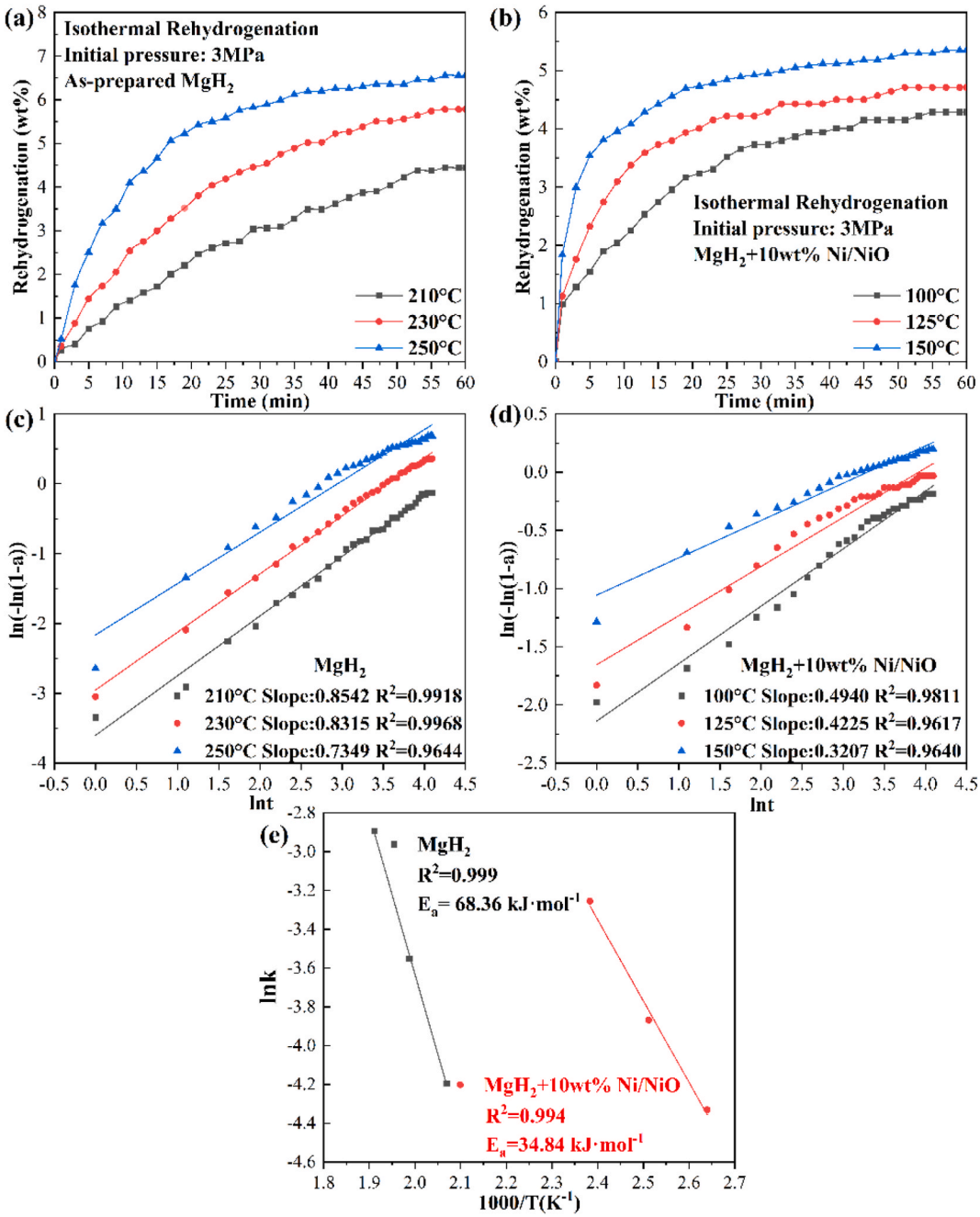

Fig. 6. Isothermal reabsorption curves of fully dehydrogenated pure MgH_2(a) and MgH_2+10 wt% Ni/NiO(b) under various temperature conditions, JMAK plots of pure MgH_2(c) and MgH_2+10 wt% Ni/NiO(d), absorption activation energy of pure MgH_2 and MgH_2+10 wt% Ni/NiO (e).

after ten cycles, the rehydrogenation value of the composite only decayed by 0.29 wt%, which indicated that the rehydrogenation performance of the composite stabilized within ten cycles. Although the quantity of hydrogen assimilated and released decreased, the final dehydrogenation and reabsorption remained at 90.22% and 95.17%. In general, MgH_2+10 wt% Ni/NiO has both rapid dehydrogenation/rehydrogenation kinetic and relatively stable cycling performance.

3.6. Catalytic mechanism of Ni/NiO on the hydrogen storage performance of MgH_2

To reveal the catalytic mechanism of Ni/NiO, transmission electron microscopy and XRD were used to study the structural changes in the composite during the dehydrogenation/rehydrogenation process.

Table 2
Absorption activation energy of Mg/MgH_2 hydrogen storage systems doped with different nickel-based catalysts.

Hydrogen storage systems	E_a (kJ/mol)	Refs.
MgH_2+10 wt% Ni/NiO	34.84	This work
MgH_2+Ni_3S_2@C-4	39.6	[29]
MgH_2+10 wt% CrFeCoNi	55.73	[30]
MgH_2+10 wt% Ni_{nps}	87.0	[32]
MgH_2+Ni@rGO	51.2	[33]
MgH_2+$Pd_{30}Ni_{70}$/CMK-3	78.5	[34]
Mg-Ni-V	52.8	[35]
Mg-5wt% NiS	45.45	[36]

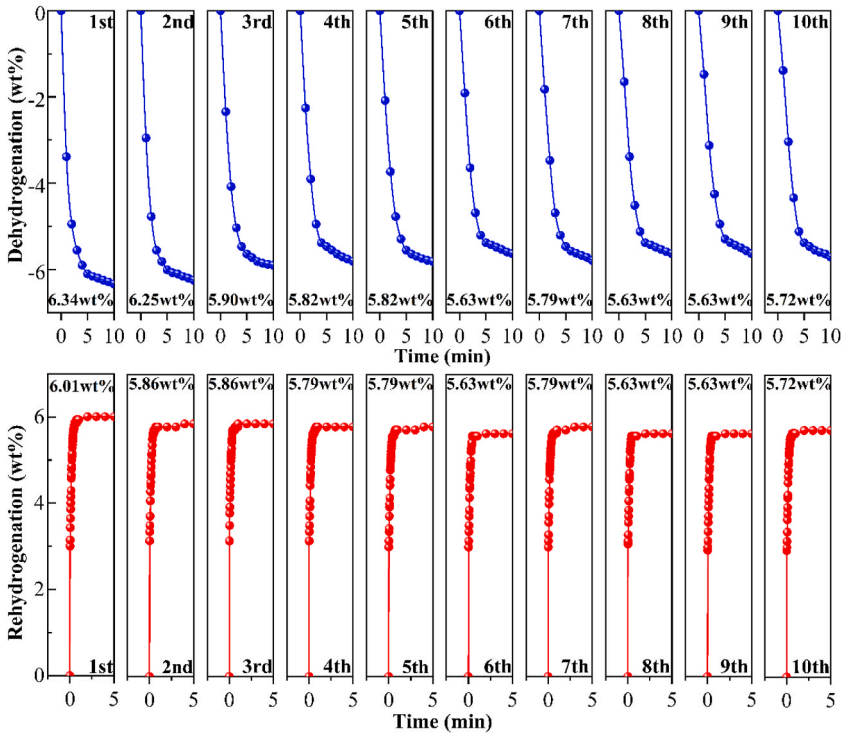

Fig. 7. Dehydrogenation/reabsorption cycle plots of MgH_2+10 wt% Ni/NiO at 320 °C.

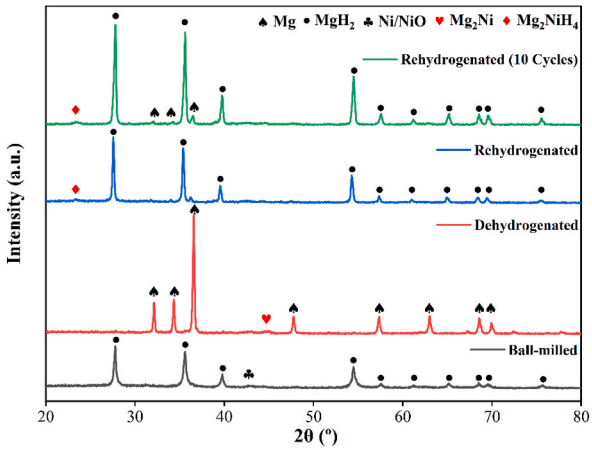

Fig. 8. XRD of MgH_2+10 wt% Ni/NiO after ball milling, dehydrogenation, hydrogen resorption, and 10 cycles.

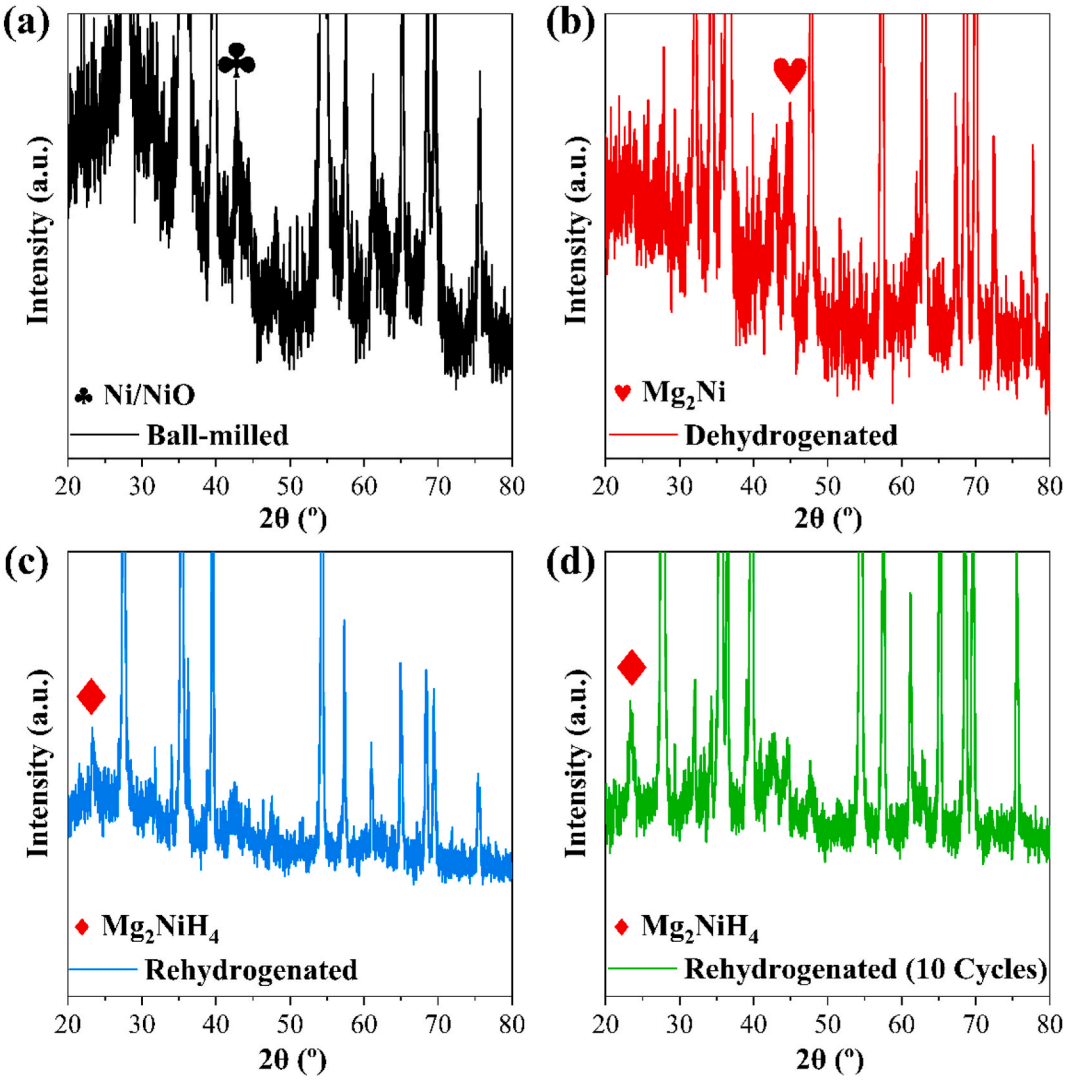

Fig. 9. XRD of Ni/NiO and its derivatives after ball milling (a), dehydrogenation (b), hydrogen resorption (c), and 10 cycles (d).

Fig. 8 shows the XRD plot of MgH_2+10 wt% Ni/NiO after ball milling, dehydrogenation, reabsorption, and 10 cycles. In addition, Fig. 9(a–d) shows the details of the catalyst and its derivatives in the XRD plots. The MgH_2 and Mg phases dominated the XRD curves. Following ball milling, the peak of Ni/NiO appeared in the MgH_2+10 wt% Ni/NiO sample, and no new phase was found, which was because there was no chemical reaction between MgH_2 and Ni/NiO, and no new species were produced. After the initial dehydrogenation, the Mg phase was dominant, and a diffraction peak of Mg_2Ni appeared. This was due to the chemical reaction between MgH_2 and Ni/NiO during the high-temperature hydrogen release process, where Ni/NiO promoted the decomposition of MgH_2 to produce hydrogen and in-situ generation of the active factor Mg_2Ni. After the initial reuptake of the sample, the diffraction peak of MgH_2 regained its dominance. It is worth mentioning that Mg_2Ni disappeared, and Mg_2NiH_4 appeared. This was because Mg_2Ni induced Mg to absorb hydrogen at high temperatures to form MgH_2, while Mg_2Ni formed Mg_2NiH_4. Mg_2Ni/Mg_2NiH_4 aided hydrogen diffusion and thus enhanced the rate of dehydrogenation and hydrogen absorption [21,29]. After 10 cycles, the MgH_2 phase was dominant, and Mg_2NiH_4 still existed because the last cycle caused Mg_2Ni to form Mg_2NiH_4 again in situ. It can be seen that Mg_2Ni and Mg_2NiH_4 are the factors for Ni/NiO to enhance the hydrogen storage capabilities of MgH_2. Mg_2Ni/Mg_2NiH_4 repeatedly switches during the dehydrogenation/rehydrogenation of composite, promoting the diffusion of hydrogen and increasing the dehydrogenation/rehydrogenation rate, which has been confirmed in many reports [21,28,29].

Fig. 10(b) shows the interplanar spacing at MgH_2(101), Ni(200), and NiO(200), recorded at distances of 0.251, 0.176, and 0.209 nm, respectively. In addition, the diffraction patterns related to MgH_2(101), Ni(200), and NiO(200) are observable in Fig. 10(c). The authenticity of the composite is further demonstrated in Fig. 10(d), where the sample's elemental composition includes Mg, Ni, and O.

To further illustrate the evolution of the Ni/NiO catalyst, Ni 2p XPS tests were performed on the MgH_2+10 wt% Ni/NiO samples after ball-milling and hydrogen release as shown in Fig. 11. The peak shapes of Ni^0 and Ni^{2+} valence states can be seen from the xps

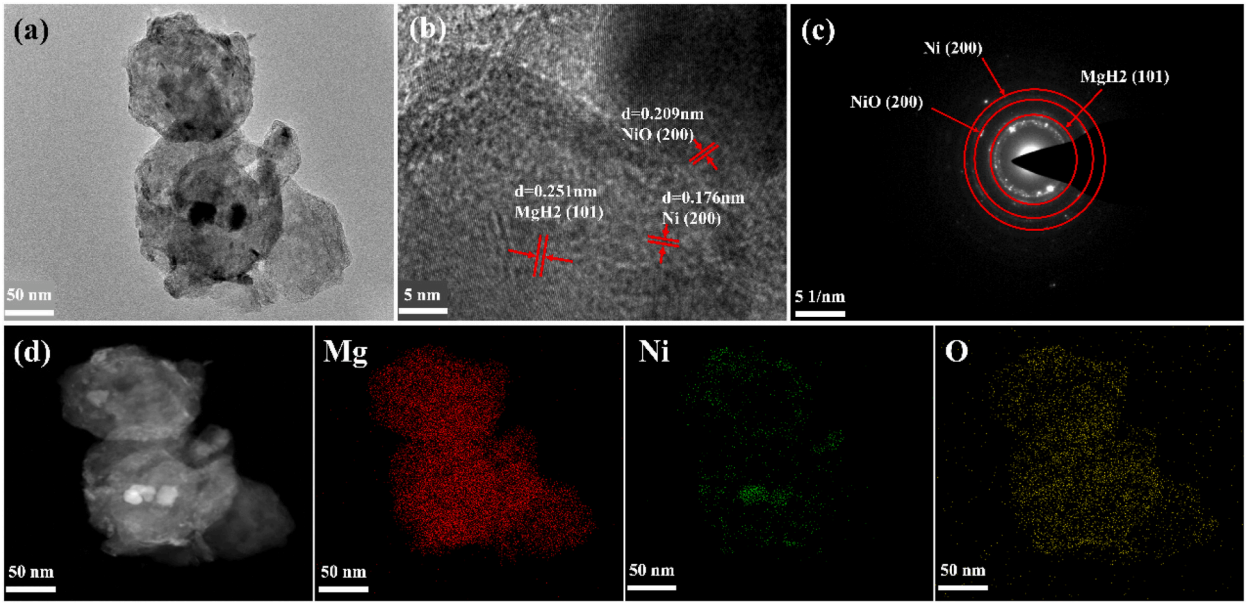

Fig. 10. TEM image (a), HRTEM image (b), SAED image (c), and EDS images (d) of MgH_2+10 wt%Ni/NiO.

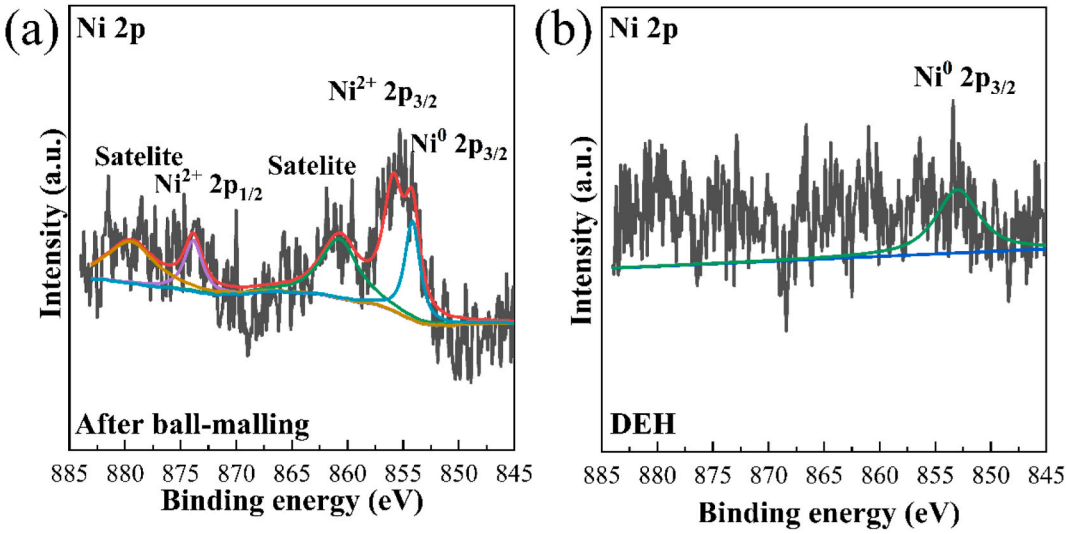

Fig. 11. Ni 2p XPS spectra of MgH_2+10 wt% Ni/NiO after ball-milling (a) and dehydrogenation (b).

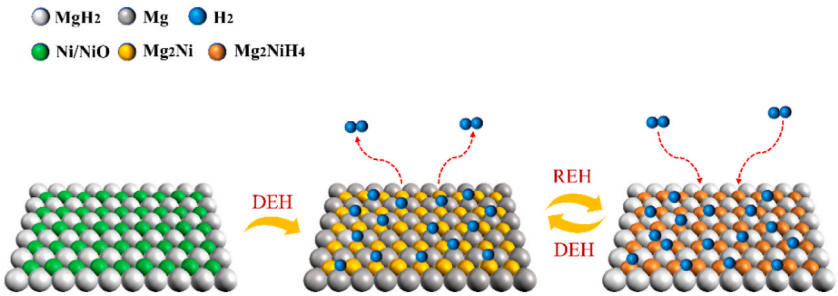

Fig. 12. Catalytic mechanism diagram of Ni/NiO catalyst.

plot of Fig. 11(a), indicating the presence of Ni and NiO in the ball-milled sample, respectively. The Ni^0 peak has a binding energy of 853 eV, and the peaks with binding energies of 855 eV and 873 eV are attributed to Ni^{2+}. After the dehydrogenation of MgH_2+10 wt% Ni/NiO, only the peak of Ni^0 is retained in the XPS plot, which is derived from the Mg_2Ni produced by the reaction of MgH_2 and Ni/NiO, which is a further confirmation of the presence of Mg_2Ni.

Combined with XRD, TEM, EDS, and other characterization images, the catalytic mechanism of Ni/NiO for MgH_2 was analyzed, as shown in Fig. 12. After ball milling, Ni/NiO was dispersed on the surface of MgH_2. Subsequently, during the initial dehydrogenation process of the composite, Ni/NiO not only assisted in the conversion of MgH_2 into Mg but also increased the hydrogen release rate and transformed it into the catalytic factor Mg_2Ni. Then, during the first rehydrogenation process, Mg_2Ni assisted in converting Mg into MgH_2, increased the reabsorption rate, and converted itself into Mg_2NiH_4. In the dehydrogenation/rehydrogenation cycles, Mg_2Ni/Mg_2NiH_4 promoted hydrogen migration across the interface of Mg/MgH_2, thereby improving the dehydrogenation/rehydrogenation kinetic of Mg/MgH_2.

4. Conclusion

Ni/NiO was synthesized by co-precipitation and introduced into MgH_2. At the same time, the excellent modification effect of the Ni/NiO on the hydrogen storage performance of MgH_2 was proved.

The dehydrogenation temperature of MgH_2+10 wt% Ni/NiO was approximately 180 °C. Moreover, the composite dehydrated 5.83 wt% within 10 min at 300 °C. The activation energies of dehydrogenation and rehydrogenation of MgH_2+10 wt% Ni/NiO were 87.21 and 34.84 kJ/mol. In the stability test of 10 cycles, the final dehydrogenation and reabsorption of MgH_2+10 wt% Ni/NiO were maintained at 90.22% and 95.17%, respectively. During the cycles of the composite system, Mg_2Ni and Mg_2NiH_4 were interconverted to promote hydrogen migration across the interface of Mg/MgH_2.

Data availability

Sharing research data helps other researchers evaluate your findings, build on your work and to increase trust in your article. We encourage all our authors to make as much of their data publicly available as reasonably possible. Please note that your response to the following questions regarding the public data availability and the reasons for potentially not making data available will be available alongside your article upon publication.

Has data associated with your study been deposited into a publicly available repository?

No.

CRediT authorship contribution statement

Wenxuan Li: Writing – review & editing, Writing – original draft. **Xinglin Yang:** Writing – review & editing. **Quanhui Hou:** Writing – review & editing. **Xiaohui Lu:** Writing – review & editing. **Jie Kong:** Writing – review & editing. **Jianye Su:** Writing – review & editing.

Declaration of competing interest

The authors declare that they have no known competing financial interests or personal relationships that could have appeared to influence the work reported in this paper.

Acknowledgements

This research was funded by the Postgraduate Research & Practice Innovation Program of Jiangsu Province (Grant No. SJCX23_2217).

References

[1] A. Gupta, G.V. Baron, P. Perreault, S. Lenaerts, R.-G. Ciocarlan, P. Cool, P.G.M. Mileo, S. Rogge, V. Van Speybroeck, G. Watson, P. Van Der Voort, M. Houlleberghs, E. Breynaert, J. Martens, J.F.M. Denayer, Hydrogen clathrates: next generation hydrogen storage materials, Energy Storage Mater. 41 (2021) 69–107.

[2] H. Liu, L. Zhang, H. Ma, C. Lu, H. Luo, X. Wang, X. Huang, Z. Lan, J. Guo, Aluminum hydride for solid-state hydrogen storage: structure, synthesis, thermodynamics, kinetics, and regeneration, J. Energy Chem. 52 (2021) 428–440.

[3] Q. Li, Y. Lu, Q. Luo, X. Yang, Y. Yang, J. Tan, Z. Dong, J. Dang, J. Li, Y. Chen, B. Jiang, S. Sun, F. Pan, Thermodynamics and kinetics of hydriding and dehydriding reactions in Mg-based hydrogen storage materials, J. Magnesium Alloys 9 (6) (2021) 1922–1941.

[4] A. Rahwanto, I. Ismail, N. Nurmalita, Mustanir, Z. Jalil, Nanoscale Ni as a catalyst in MgH2 for hydrogen storage material, J. Phys. Conf. 1882 (1) (2021) 012010.

[5] L. Zhang, L. Ji, Z. Yao, N. Yan, Z. Sun, X. Yang, X. Zhu, S. Hu, L. Chen, Facile synthesized Fe nanosheets as superior active catalyst for hydrogen storage in MgH2, Int. J. Hydrogen Energy 44 (39) (2019) 21955–21964.

[6] R.R. Shahi, A. Bhatnagar, S.K. Pandey, V. Dixit, O.N. Srivastava, Effects of Ti-based catalysts and synergistic effect of SWCNTs-TiF3 on hydrogen uptake and release from MgH2, Int. J. Hydrogen Energy 39 (26) (2014) 14255–14261.

[7] J. Liu, Z. Ma, Z. Liu, Q. Tang, Y. Zhu, H. Lin, Y. Zhang, J. Zhang, Y. Liu, L. Li, Synergistic effect of rGO supported Ni3Fe on hydrogen storage performance of MgH2, Int. J. Hydrogen Energy 45 (33) (2020) 16622–16633.

[8] S. Gao, X. Wang, H. Liu, T. He, Y. Wang, S. Li, M. Yan, CNTs decorated with CoFeB as a dopant to remarkably improve the dehydrogenation/rehydrogenation performance and cyclic stability of MgH2, Int. J. Hydrogen Energy 45 (53) (2020) 28964–28973.
[9] M. Song, L. Zhang, J. Zheng, Z. Yu, S. Wang, Constructing graphene nanosheet-supported FeOOH nanodots for hydrogen storage of MgH2, Int. J. Miner. Metall. Mater. 29 (7) (2022) 1464–1473.
[10] G. Liu, L. Wang, Y. Hu, C. Sun, H. Leng, Q. Li, C. Wu, Enhanced catalytic effect of TiO2@rGO synthesized by one-pot ethylene glycol-assisted solvothermal method for MgH2, J. Alloys Compd. 881 (2021) 160644.
[11] Q. Meng, Y. Huang, J. Ye, G. Xia, G. Wang, L. Dong, Z. Yang, X. Yu, Electrospun carbon nanofibers with in-situ encapsulated Ni nanoparticles as catalyst for enhanced hydrogen storage of MgH2, J. Alloys Compd. 851 (2021) 156874.
[12] P.K. Soni, A. Bhatnagar, V. Shukla, M.A. Shaz, Improved de/re-hydrogenation properties of MgH2 catalyzed by graphene templated Ti-Ni–Fe nanoparticles, Int. J. Hydrogen Energy 47 (50) (2022) 21391–21402.
[13] L. Dan, H. Wang, J. Liu, L. Ouyang, M. Zhu, H2 plasma reducing Ni nanoparticles for superior catalysis on hydrogen sorption of MgH2, ACS Appl. Energy Mater. 5 (4) (2022) 4976–4984.
[14] G. Liu, F. Qiu, J. Li, Y. Wang, L. Li, C. Yan, L. Jiao, H. Yuan, NiB nanoparticles: a new nickel-based catalyst for hydrogen storage properties of MgH2, Int. J. Hydrogen Energy 37 (22) (2012) 17111–17117.
[15] Q. Zhang, L. Zang, Y. Huang, P. Gao, L. Jiao, H. Yuan, Y. Wang, Improved hydrogen storage properties of MgH2 with Ni-based compounds, Int. J. Hydrogen Energy 42 (38) (2017) 24247–24255.
[16] S. Ren, Y. Fu, L. Zhang, L. Cong, Y. Xie, H. Yu, W. Wang, Y. Li, L. Jian, Y. Wang, S. Han, An improved hydrogen storage performance of MgH2 enabled by core-shell structure Ni/Fe3O4@MIL, J. Alloys Compd. 892 (2022) 162048.
[17] J. Wu, H. Zhang, Y. Wang, Y. Zou, B. Li, C. Xiang, L. Sun, F. Xu, T. Yu, Hydrangea-like NiO@KNbO3 as catalyst doping for MgH2: boosting hydrogen storage performance, J. Alloys Compd. 961 (2023) 171160.
[18] C. Duan, Y. Tian, X. Wang, M. Wu, D. Fu, Y. Zhang, W. Lv, Z. Su, Z. Xue, Y. Wu, Ni-CNTs as an efficient confining framework and catalyst for improving dehydriding/rehydriding properties of MgH2, Renew. Energy 187 (2022) 417–427.
[19] Z. Yu, X. Liu, Y. Liu, Y. Li, Z. Zhang, K. Chen, S. Han, Synergetic catalysis of Ni@C@CeO2 for driving ab/desorption of MgH2 at moderate temperature, Fuel 357 (2024) 129726.
[20] Q. Hou, J. Zhang, G. XinTao, G. Xu, X. Yang, Synthesis of low-cost biomass charcoal-based Ni nanocatalyst and evaluation of their kinetic enhancement of MgH2, Int. J. Hydrogen Energy 47 (34) (2022) 15209–15223.
[21] Q. Hou, X. Yang, J. Zhang, W. Yang, E. Lv, Catalytic effect of NiO/C derived from Ni-UMOFNs on the hydrogen storage performance of magnesium hydride, J. Alloys Compd. 899 (2022) 163314.
[22] S.K. Mohamed, A.M. Elhgrasi, O.I. Ali, Facile synthesis of mesoporous nano Ni/NiO and its synergistic role as super adsorbent and photocatalyst under sunlight irradiation, Environ. Sci. Pollut. Res. Int. 29 (43) (2022) 64792–64806.
[23] X. Yang, Q. Hou, L. Yu, J. Zhang, Improvement of the hydrogen storage characteristics of MgH2 with a flake Ni nano-catalyst composite, Dalton Trans. 50 (5) (2021) 1797–1807.
[24] Z. Ding, L. Zhang, Y. Fu, W. Wang, Y. Wang, J. Bi, Y. Li, S. Han, Enhanced kinetics of MgH2 via in situ formed catalysts derived from MgCCo1.5Ni1.5, J. Alloys Compd. 822 (2020) 153621.
[25] J. Zhang, L. He, Y. Yao, X.J. Zhou, L.P. Yu, X.Z. Lu, D.W. Zhou, Catalytic effect and mechanism of NiCu solid solutions on hydrogen storage properties of MgH2, Renew. Energy 154 (2020) 1229–1239.
[26] J. Zhang, Q. Hou, J. Chang, D. Zhang, Y. Peng, X. Yang, Improvement of hydrogen storage performance of MgH2 by MnMoO4 rod composite catalyst, Solid State Sci. 121 (2021) 106750.
[27] M.S. El-Eskandarany, E. Shaban, H. Al-Matrouk, M. Behbehani, A. Alkandary, F. Aldakheel, N. Ali, S.A. Ahmed, Structure, morphology and hydrogen storage kinetics of nanocomposite MgH2/10 wt% ZrNi5 powders, Mater. Today Energy 3 (2017) 60–71.
[28] Q. Hou, J. Zhang, X. Guo, X. Yang, Improved MgH2 kinetics and cyclic stability by fibrous spherical NiMoO4 and rGO, J. Taiwan Inst. Chem. Eng. 134 (2022) 104311.
[29] L. Zeng, Z. Lan, B. Li, H. Liang, X. Wen, X. Huang, J. Tan, H. Liu, W. Zhou, J. Guo, Facile synthesis of a Ni3S2@C composite using cation exchange resin as an efficient catalyst to improve the kinetic properties of MgH2, J. Magnesium Alloys 10 (12) (2022) 3628–3640.
[30] L. Wang, L. Zhang, X. Lu, F. Wu, X. Sun, H. Zhao, Q. Li, Surprising cocktail effect in high entropy alloys on catalyzing magnesium hydride for solid-state hydrogen storage, Chem. Eng. J. 465 (2023) 142766.
[31] C. Hu, Z. Zheng, T. Si, Q. Zhang, Enhanced hydrogen desorption kinetics and cycle durability of amorphous TiMgVNi3-doped MgH2, Int. J. Hydrogen Energy 47 (6) (2022) 3918–3926.
[32] S. Wang, M. Gao, Z. Yao, K. Xian, M. Wu, Y. Liu, W. Sun, H. Pan, High-loading, ultrafine Ni nanoparticles dispersed on porous hollow carbon nanospheres for fast (de)hydrogenation kinetics of MgH2, J. Magnesium Alloys 10 (12) (2022) 3354–3366.
[33] Z. Lan, L. Zeng, G. Jiong, X. Huang, H. Liu, N. Hua, J. Guo, Synthetical catalysis of nickel and graphene on enhanced hydrogen storage properties of magnesium, Int. J. Hydrogen Energy 44 (45) (2019) 24849–24855.
[34] H. Cheng, G. Chen, Y. Zhang, Y. Zhu, L. Li, Boosting low-temperature de/re-hydrogenation performances of MgH2 with Pd-Ni bimetallic nanoparticles supported by mesoporous carbon, Int. J. Hydrogen Energy 44 (21) (2019) 10777–10787.
[35] X. Xie, M. Chen, P. Liu, J. Shang, T. Liu, Synergistic catalytic effects of the Ni and V nanoparticles on the hydrogen storage properties of Mg-Ni-V nanocomposite, Chem. Eng. J. 347 (2018) 145–155.
[36] X. Xie, X. Ma, P. Liu, J. Shang, X. Li, T. Liu, Formation of multiple-phase catalysts for the hydrogen storage of Mg nanoparticles by adding flowerlike NiS, ACS Appl. Mater. Interfaces 9 (7) (2017) 5937–5946.